Hints of FLRW breakdown from supernovae

Chethan Krishnan,[1,*] Roya Mohayaee,[2,†] Eoin Ó Colgáin,[3,4,‡] M. M. Sheikh-Jabbari,[5,§] and Lu Yin[3,4,‖]

[1]*Center for High Energy Physics, Indian Institute of Science, Bangalore 560012, India*
[2]*Sorbonne Université, CNRS, Institut d'Astrophysique de Paris, 98bis Bld Arago, Paris 75014, France*
[3]*Center for Quantum Spacetime, Sogang University, Seoul 121-742, Korea*
[4]*Department of Physics, Sogang University, Seoul 121-742, Korea*
[5]*School of Physics, Institute for Research in Fundamental Sciences (IPM), P.O.Box 19395-5531, Tehran, Iran*

(Received 14 July 2021; revised 29 September 2021; accepted 22 February 2022; published 11 March 2022)

A 10% difference in the scale for the Hubble parameter constitutes a clear problem for cosmology. Here, considering angular distribution of type Ia supernovae (SN) within the Pantheon compilation and working within flat ΛCDM cosmology, we observe a correlation between higher H_0 and the CMB dipole direction, confirming our previous results for strongly lensed quasars [Classical Quantum Gravity **38**, 184001 (2021)]. Concretely, we record a ∼1 km/s/Mpc variation in H_0 at antipodal points on the sky within the Pantheon sample, which is evident in the Low z subsample ($z \lesssim 0.075$) and gets enhanced by higher redshift SN. Our work raises the possibility that we may be at the precision required to probe anisotropic Hubble expansions, while providing a concrete prediction for future inferences of H_0.

DOI: 10.1103/PhysRevD.105.063514

I. INTRODUCTION

Systematics aside (most recently [1,2]), Hubble tension is a ∼10% discrepancy in the Hubble constant H_0 between an early Universe determination based on the flat ΛCDM model [3] and late Universe determinations based on the distance ladder [4,5]. To date, the search for cosmological solutions has been almost exclusively restricted to the Friedmann-Lemaître-Robertson-Walker (FLRW) paradigm [6]. We recently laid bare the limitations of this approach by providing a ballpark figure for the maximum H_0 achievable within any FLRW cosmology [7] (see also [8]):

$$H_0 \sim 71 \pm 1 \text{ km/s/Mpc}, \tag{1.1}$$

subject to the proviso that one works within general relativity [9]. We stress that this maximum H_0 can only be achieved if one allows an alteration of the sound horizon with new early Universe physics. Evidently, local determinations of $H_0 \sim 73$ km/s/Mpc can be tolerated within 2σ, provided one ignores the tendency of new early Universe physics [11–14] to exacerbate σ_8 tension [15–22].

Over the last decade, we have witnessed a steady stream of independent studies ranging from radio galaxies [23–30] to quasars (QSOs) [31] showing that dipoles associated with CMB and distribution of large structures do not match at large redshifts $z \gtrsim 1$ (even at 4.9σ [31]) (see also 32,33]]). Throughout, the claims have been consistent that the dipole agrees with the CMB dipole in direction, but not magnitude. Once again, systematics could be at play, but it is worth noting that the redshift range is well beyond where peculiar velocities and local bulk flows are relevant [34]. Separately, it has been noted in galaxy cluster scaling relations [36,37] that H_0 may track the CMB dipole. Moreover, even with Planck CMB data, flat ΛCDM cosmological parameters exhibit dipoles close to the CMB dipole [38]. If true, this may point to a misinterpretation of the CMB dipole within modern cosmology. Simply put, observables should not track the CMB dipole when in CMB frame.

Furthermore, it was recently observed [7] that H_0 values inferred from strongly lensed QSOs within the flat ΛCDM model [39,40] appeared to be correlated with the CMB dipole direction. The same observation extends to oCDM and wCDM models [39]. We illustrate this trend in Fig. 1, where we plot H_0 values against galaxy counts from the 2MRS catalog [41], where the latter gives an indication of structure in the local Universe. There are three plausible explanations for Fig. 1:

(1) This is a manifestation of a breakdown in FLRW at large redshift in line with persistent disagreement in the dipoles [23–31].
(2) Local structure along the line of sight could be playing a role [42], underscoring a need to better model known superclusters when inferring H_0 from strong lensing

*chethan.krishnan@gmail.com
†mohayaee@iap.fr
‡ocolgain@gmail.com
§shahin.s.jabbari@gmail.com
‖yinlu@sogang.ac.kr

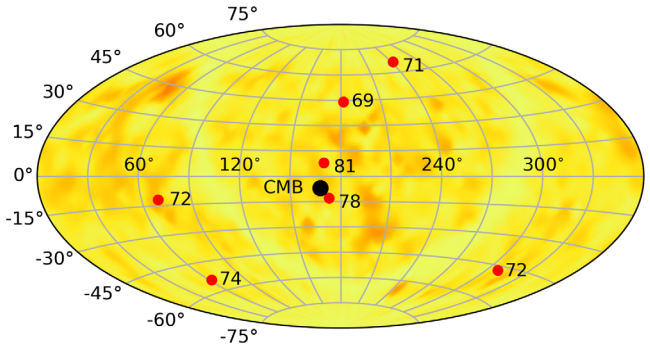

FIG. 1. H_0 values from strongly lensed QSOs alongside the CMB dipole against a background of 2MRS galaxy counts. These galaxies are relatively local and the observed anisotropies in 2MRS have to extend to much higher redshifts for them to have a significant impact on the strong lensing measurements of the Hubble parameter.

time delay [39,40]. Since the QSOs are deep in redshift, while the 2MRS catalog in Fig. 1 is more local, one does not expect any immediate correlation.

(3) This could be a coincidence.

Already the balance may be tipped in favor of option 1, but here we support the observation further through type Ia supernovae (SN). Recall that Cooke and Lynden-Bell have already noted the presence of a small increase in the cosmic acceleration for the union compilation of type Ia SN [45] in the direction $(198°, -20°)$ [46]. As emphasized in the original work [46], the effect is small $(\sim 1\sigma)$, but it is apparent at higher redshifts, $z > 0.53$, where it could overlap with any anisotropy traced by QSOs. The main thrust of this short note is to revisit and reinforce this observation with the Pantheon dataset [47].

II. ANALYSIS

Before beginning, let us interpret Fig. 1 as a statistical fluke in order to quantify how often this can happen. To do so, choose the CMB dipole direction, with right ascension $\mathcal{R}$ and declination $\mathcal{D}$, $(\mathcal{R}, \mathcal{D}) = (168°, -7°)$. For each angle in Table IV of [7], construct the vector,

$$\vec{v} = (\cos\mathcal{D}\cos\mathcal{R}, \cos\mathcal{D}\sin\mathcal{R}, \sin\mathcal{D}). \tag{2.1}$$

Next, split the seven lenses into two hemispheres using the sign of the inner product of the CMB dipole direction vector with the lens vector. In each hemisphere A and B, one can identify a weighted average H_0 [48], before identifying the H_0 discrepancy:

$$\sigma := \frac{(H_0^A - H_0^B)}{\sqrt{(\delta H_0^A)^2 + (\delta H_0^B)^2}}. \tag{2.2}$$

Concretely, we find $\sigma = 1.18$ for the real sample. To find out how representative this number is, we shift all lenses to their weighted averaged $H_0 = 73.53 \pm 1.46$ km/s/Mpc, and generate 100,000 copies of the original H_0 in a normal distribution using the H_0 error for each lens. Repeating the steps above, in 12% of the configurations one finds a larger value of σ, so the probability of a fluke is $p = 0.12$. This may seem small compared to $\sigma = 1.18$, but note that σ is a difference in weighted averages and the weighted averages have further internal freedoms. We have also repeated the exercise while weighting the H_0 values for both errors and orientation with respect to the CMB dipole, thereby bringing it more into line with later analysis. The difference was negligible, simply reducing $p = 0.12$ to $p = 0.116$.

Next we move to Pantheon type Ia SN, where we take all corrections for peculiar velocities at face value. The redshifts have been corrected for the local-group motion and are in the CMB rest frame (e.g. they are not heliocentric redshifts). We refer the readers to [49–53] for previous studies using SN to test the cosmological principle and to [54,55] for studies within Pantheon compilation and also to [56–58] for the impact of peculiar velocities on nearby SN. In contrast to previous studies [54,55], here we follow the intuition from Fig. 1 and [46] that the CMB dipole direction is most relevant. It should be stressed that it is *assumed* the CMB dipole is simply due to relative motion, but an intrinsic dipole cannot yet be ruled out, (see e.g. [59]). Here, with limited assumptions we will show that a dipole emerges from the Pantheon dataset, *despite the "sample" apparently being cleaned for peculiar motions and being in the same rest frame as the CMB*. We first focus on the entire sample, which includes 1048 SN in the redshift range $0.01 < z \leq 2.26$ [60].

Our analysis is similar to [62], but we focus on H_0 rather than matter density Ω_{m0}, since this is the most precisely constrained parameter by SN data, even at low redshifts, and it is the relevant parameter from Fig. 1. We work within the flat ΛCDM model and since H_0 and Ω_{m0} are negatively correlated, we have confirmed that scans for differences in Ω_{m0} produce similar results. As emphasized in [63], H_0 is an integration constant that is universal to *all* FLRW cosmologies, whereas Ω_{m0} is a model dependent parameter. For this reason, we expect trends in H_0 to generalize to *all* FLRW cosmologies, but obviously the significance will depend on the number of model parameters.

We divide the sky up into a 31×15 grid for $\mathcal{R}$ and $\mathcal{D}$ in the ranges $0 \leq \mathcal{R} \leq 2\pi$ and $-\pi/2 \leq \mathcal{D} \leq \pi/2$. Note, there is some redundancy in the points at the boundaries of $\mathcal{R}$ and at the poles [64]. By opting for an odd number of points, we include the antipodal points on the sky, and as is clear from (2.1), by flipping the sign of $\mathcal{D}$ and shifting $\mathcal{R} \to \mathcal{R} \pm \pi$ one gets the antipodal point. For each point on the sky, we convert it to a vector $\vec{v}$ (2.1) and do the same for all the SN in the sample $\vec{v}_i$. Next, we split the SN according to the sign of the inner product $\vec{v} \cdot \vec{v}_i$. SN with positive sign are in the hemisphere aligned with $\vec{v}$, whereas those with the negative sign are in the opposite hemisphere.

One then fits the flat ΛCDM model in both hemispheres and identifies any discrepancy (2.2), before repeating for all points on the sky. In performing the fitting, we make use of the full Pantheon covariance matrix [65], i.e. both statistical and systematic uncertainties. The latter takes the form of a covariance matrix [47], which we crop accordingly to restrict to SN in a given hemisphere.

The result of the above exercise is shown in Fig. 2. Note that we have performed a cubic interpolation between points, using the python scipy library (scipy.interpolate.griddata) to improve presentation, but we only quote results for points where we have performed fitting. As is clear from the plot, the higher values of H_0 (red regions) are in hemispheres aligned with the CMB dipole. The maximum value of $\sigma = 1.7$ is found at $(216°, -64.3°)$. Thus, by symmetry, the minimum value of $\sigma = -1.7$ is at $(36°, +64.3°)$. In contrast, in the CMB dipole direction σ is lower, $\sigma = 0.39$. However, it should be stressed that H_0 is more or less model agnostic within FLRW cosmologies and is one of the bluntest probes of anisotropy, since it has no directional dependence. Therefore, the main take away is the separation of the sky into higher H_0 and lower H_0 directions with the CMB dipole direction corresponding to a region of higher H_0. When phrased in absolute values, $\sim 1.5\sigma$ equates to a $\Delta H_0 \sim 1$ km/s/Mpc ($\Delta m_B \sim 0.03$ mag) differential at antipodal points on the sky. This is comparable to the latest SH0ES H_0 errors [66].

A number of comments are in order. First, we can view the most pronounced differences as a departure from FLRW, admittedly at low statistical significance. We can compare this intrinsic $\sim 1.5\sigma$ dipole to a kinematic dipole by boosting the Pantheon redshifts to heliocentric frame following [67]. We have checked that this produces a stronger dipole at $\sim 4.5\sigma$. For smaller kinematic velocities $v_0 < 369.82$ km/s, we find that the feature is rotated on the sky and cannot be removed by changing the magnitude of our relative velocity. Nevertheless, the trend in H_0 is consistent with Fig. 1. Second, the orientation is consistent with the results of [23–31,68] in the sense that there is an unexpected dipole even though Pantheon SN are in the *same frame* as the CMB. This effect, if physical, can potentially be traced to the difference in magnitude in the cosmic dipole reported in [23–31].

The Pantheon sample comprises Low z [69–76] (172 SN), SDSS (335 SN) [77–79], PS1 (279 SN) [80,81], SNLS (236 SN) [82,83], and HST (26 SN) subsamples [84–89], with mean redshifts $\bar{z} = 0.03, 0.20, 0.29, 0.64$ and 1.27, respectively (see [47], Fig. 10). However, neglecting the Low z subsample, sky coverage is patchy: SDSS is exclusively in the hemisphere opposite to the CMB dipole, whereas PS1 covers 10 directions and SNLS samples 4 directions on the sky (3 of which are common to PS1). We have checked that only the removal of the Low z subsample ($0.01 < z \leq 0.07515$) drastically affects Fig. 2. In short, while the other subsamples contribute to Fig. 2, the Low z sample is central. Intuitively, this may have a simple explanation in the much better sky coverage. In Fig. 3 we plot the same feature from the Low z sample. Evidently, high redshift SN enhance the feature. It is worth noting that any residual dipole in the Low z sample shows consistent directional dependence with reported anomalous bulk flows [57,90–92], which have most recently been recovered in Ref. [93]. Since we are working at low redshift, we have fixed $\Omega_{m0} = 0.3$. This restriction makes little difference as with fixed Ω_{m0}, errors no longer propagate and differences in H_0 between hemispheres are still $\Delta H_0 \sim 1$ km/s/Mpc.

Now comes the interesting question: how likely is Fig. 2 as a statistical fluke? Before addressing this point, note that an *a priori* exploration of the CMB dipole direction is well motivated, since it represents the unique direction of motion of the local group with respect to the CMB. Moreover, a number of studies [30,31,46] have reported anisotropies in matter in directions consistent with the CMB dipole direction. If there is a dipole in matter that differs from the CMB dipole, it would be surprising if it exactly aligned, but close alignment may happen. Here, we use the CMB dipole direction within our local frame as an *a priori* input in order to quantify the statistical significance of any departure from expected flat ΛCDM behavior.

We essentially repeat the process leading to Fig. 2, but using a coarser sky grid 11×5. Once one accounts for

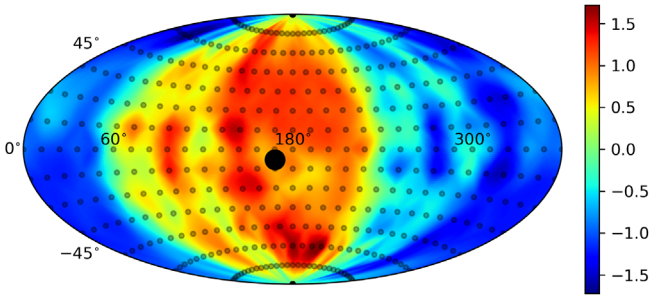

FIG. 2. Variation in the discrepancy in H_0 (σ) across the sky for the full Pantheon SN dataset. The large black dot denotes the CMB dipole direction, while the smaller black dots show points on the sky where we have directly fitted flat ΛCDM prior to interpolation.

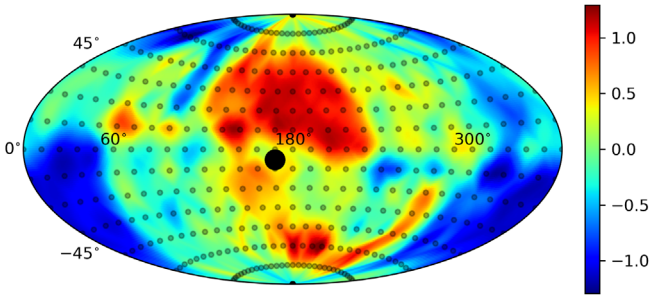

FIG. 3. Variation in the discrepancy in H_0 (σ) across the sky for the Low z subsample ($0.01 < z \leq 0.07515$). The large black dot denotes the CMB dipole direction, while the smaller black dots show points on the sky where we have directly fitted flat ΛCDM prior to interpolation.

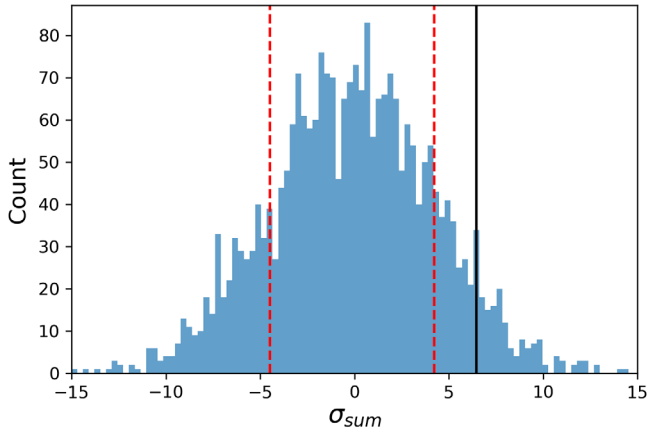

FIG. 4. The distribution of the weighted sum across 2500 mock realizations of the Pantheon dataset. Red dotted lines denote 1σ, while the black line represents the value for the real data.

boundaries, this leaves 50 independent, evenly spaced points on the sky. By symmetry, 25 of these points are in the same hemisphere as the CMB dipole direction. For each of these 25 points, we identify a σ_i (2.2), which we sum, but weighted according to the inner product of that direction on the sky with the CMB dipole direction, i.e.

$$\sigma_{\rm sum} = \sum_i (\vec{v}_i \cdot \vec{v}_{\rm dipole})\sigma_i. \tag{2.3}$$

This projects the 25 σ_i's onto the CMB dipole direction, so that the points on the sky that are more closely aligned contribute more. The role of the weighted sum is to allow freedom in any putative matter dipole, while still focusing on directions close to the CMB dipole.

For the real data, we find $\sigma_{\rm sum} = 6.471$, which one can compare to mock realizations of the data. To do so, we fit the flat ΛCDM model to the original data and extract best-fit values, $H_0 = 70.03 \pm 0.35$ km/s/Mpc, $\Omega_{m0} = 0.298 \pm 0.022$, and a corresponding 2×2 covariance matrix. Note that throughout we fix the absolute magnitude M of SN to a nominal constant value so that $H_0 \sim 70$ km/s/Mpc for the overall dataset. Moreover, in fitting flat ΛCDM, we confirm the best-fit value of matter density from Table 8 of [47]. This serves as a rudimentary consistency check. From the covariance matrix, we draw a normal distribution of 2500 (H_0, Ω_{m0}) pairs, and for each pair, we generate values of apparent magnitude m_B using the full covariance matrix of the Pantheon dataset. For each realization, we repeat the scan over the sky, identify σ_i at 25 points, before identifying the corresponding weighted sum. We find a weighted sum exceeding the real data value in 162 from 2500 realizations, thus corresponding to a probability of $p = 0.065$. The resulting distribution of $\sigma_{\rm sum}$ is shown in Fig. 4.

III. OUTLOOK

As explained in [7], a resolution to Hubble tension within a FLRW cosmology requires the introduction of new early Universe physics. This is currently the front-running idea. However, it has become apparent that early Universe resolutions to Hubble tension typically exacerbate other discrepancies [15–22]. Moreover, it should be stressed that the introduction of new early Universe physics has only one real motivation, essentially to bring the baryon acoustic oscillation (BAO) scale into line with Cepheid-calibrated SN, with no distinctive prediction. In physics, results lying on a single motivating observation, and without a predictive signature, are weak (even when they work).

On the other hand, discrepancies between the CMB dipole and dipoles attributable to distant sources, namely radio galaxies [23–30] and QSOs [31], have persisted for over a decade. These data are mostly at very high redshifts well beyond the redshifts where peculiar velocities/bulk flows can matter in FLRW.

The correlation in Fig. 1, originally observed in [7], may constitute a fluke with probability $p = 0.12$. Combining this with the probability we obtained here with Pantheon type Ia SN [47], using Fisher's method and noting that the strong lensing results (Fig. 1) and our present SN results (Fig. 2) are statistically independent, yields $p = 0.046$, or alternatively, 1.7σ. The lensed QSO result, while low in statistical significance, is unlikely to be the result of some local effects, since the lenses and the QSOs are much deeper in redshift. Moreover, the consistency of SN and lensed QSO results with similar results in high redshift probes [94], makes it considerably less likely that our feature is a statistical fluke.

Certainly, Fig. 2 is unexpected, since the Pantheon SN compilation has been put in CMB frame by construction, so any residual variation in H_0, especially one in the direction of the CMB dipole, is striking. While the various subsamples of Pantheon contribute to this feature, it is robust to the removal of all subsamples, except the Low z subsample. Tellingly, this sample has the best sky coverage. Evidently, Fig. 2 has other contributions beyond simply the Low z subsample, but low redshift SN appear to play a key role (see also [56,95–98]). Finally, it should be stressed that since we work within flat ΛCDM any approach is minimal and a "fundamental constant" within the FLRW paradigm, namely H_0, is under the spotlight.

Anisotropy in the Hubble parameter has previously been reported for the Union II dataset [46]. Even prior to that and back in 2007 McClure and Dyer reported a statistically significant *local* anisotropy in the value of Hubble parameter [99]. They used a single dataset from HST key project and are hence clean of systematics typical of composite datasets. That the Hubble parameter is locally anisotropic is not under question: local anisotropy in the Hubble value is usually absorbed into the peculiar velocities in perturbation analysis. The question is why such an anisotropy seems to persist in spite of Pantheon having undergone extensive cleaning for the local flow. The perhaps more fundamental question is why such an anisotropy seems to persist to high redshifts. This is totally unexpected in an FLRW Universe.

In summary, there are a number of takeaways. Results from strong lensing data (Fig. 1) and SN data (Fig. 2) are consistent, thereby providing a concrete prediction for future H_0 probes (e.g. [94]). Second, our SN analysis (Fig. 2) shows both a low redshift and a high redshift effect, one which is not easily removed by changing the magnitude of our velocity with respect to CMB. Finally, $\Delta H_0 \sim 1$ km/s/Mpc is already at the level of precision of the latest SH0ES determination [66], which ultimately means that we may already be at a requisite precision to take anisotropic Hubble expansions seriously.

ACKNOWLEDGMENTS

We thank Lucas Macri for correspondence. We thank Nikki Arendse, Angela Chen, Adrià Gomez-Valent, Jackson Said, and Joan Solà for feedback on an earlier draft. We are also grateful to anonymous referees for helping us sharpen our presentation. E. Ó. C. is funded by the National Research Foundation of Korea (Grant No. NRF-2020R1A2C1102899). M. M. S.-J. would like to acknowledge Saramadan Grant No. ISEF/M/400122. L. Y. was supported by the National Research Foundation of Korea funded through the CQUeST of Sogang University (Grant No. NRF-2020R1A6A1A03047877).

APPENDIX: ROBUSTNESS OF OBSERVATION

In this section, we provide some plots to show how the feature in Fig. 2 changes as we remove SN subsamples. We begin with Fig. 5 where we show the distribution of SN when decomposed into Low z (172 SN), PS1 (279 SN), SDSS (335 SN), SNLS (236 SN), and HST SN (26 SN) subsamples. Understandably, as one moves to higher redshift, the sky coverage becomes pretty poor, but once seen, this is intuitive. The SDSS subsample (blue) is exclusively in the hemisphere opposite to the CMB dipole. Moreover, PS1 (green) covers only 10 (isolated) directions on the sky, while SNLS covers 4 (magenta) directions, of which 3 are common to PS1. In short, beyond Low z, the sky coverage is pretty poor. That being said, if the Universe is FLRW, this makes no difference. Observe also that there are relatively few SN in the lower hemisphere, whereas we are seeing a clear signal from that part of the sky in Fig. 2. The differences we report are between hemispheres, so they may be driven by SN in the opposite direction.

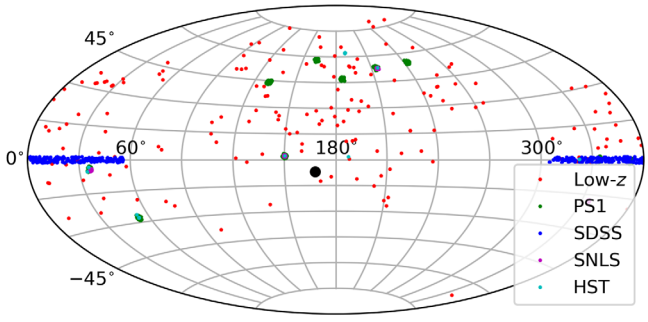

FIG. 5. Location of SN on the sky according to Pantheon subsample.

Next, we have repeated our scan by omitting each subsample in turn and, as expected, the most pronounced effect is found when the Low z sample ($z \lesssim 0.075$) is removed. As is clear from Fig. 6, when the Low z sample is removed, the dipole changes dramatically and one is no longer tracking the CMB dipole direction. Nevertheless, if one retains the Low z sample, but removes the SDSS sample, which is the subsample with the next lowest effective redshift, one finds the feature in Fig. 7. One can see that with Low z, but without SDSS, the plot starts to resemble Fig. 2 in the sense that one is seeing variations in H_0 with greater significance, but still the feature is not so pronounced, yet evidently more pronounced than when only considers the Low z sample in Fig. 3. Removing higher redshift samples beyond SDSS, namely PS1, SNLS or HST make very little difference, so we omit the plots. One interpretation of these results is that H_0 variations are mainly coming from Low z sample, but the contributions from PS1, SDSS, SNLS, and HST reinforce it. Let us stress that if there is a matter anisotropy aligned with the CMB dipole direction, then one will need SN samples with better overlap with these directions (see Fig. 5) to definitively confirm that higher redshift SN enhance the feature.

Finally, we have performed some additional checks. Pantheon quotes both CMB redshifts $z_{\rm CMB}$, some of which we have checked agree with the earlier JLA sample, but there are further corrected Hubble diagram redshifts, z_{HD}.

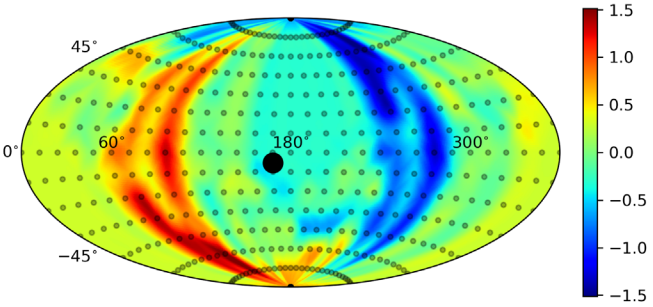

FIG. 6. Same as Fig. 2 of manuscript but with Low z removed.

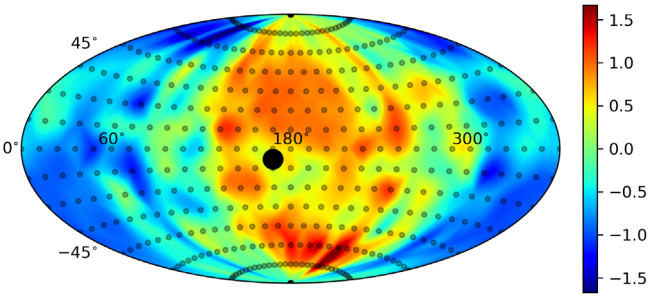

FIG. 7. Same as Fig. 2 of manuscript but with SDSS removed.

The difference appears to be whether one corrects for any peculiar motion of the source SN, or not. These z_{HD} are the redshifts that recover the cosmological parameters in the Pantheon paper [47]. We have checked that whether one uses $z_{\rm CMB}$ or z_{HD}, Fig. 2 in the manuscript is the same. One can also remove the systematic uncertainties from Pantheon, but this does not qualitatively change our Fig. 2. One still finds $\sim 1.5\sigma$ discrepancies in certain directions on the sky. Nevertheless, boosting from CMB frame (starting from $z_{\rm CMB}$) to heliocentric frame following Eq. (7) of Ref. [67], the significance increases by $\sim 4.5\sigma$. To see this, note that we have an intrinsic dipole at $\sim 1.5\sigma$ in Fig 2. of the draft, while in Fig. 8, the colors are reversed at $\sim 3\sigma$. This highlights the difference between the residual feature we see in Pantheon in *CMB frame* (by construction) and a kinematic feature. A kinematic feature is expectedly stronger. So one of the take away messages of the manuscript is that despite all the corrections, Pantheon still has an intrinsic or residual dipole in the direction of the CMB dipole. This appears consistent with the lenses presented in Fig. 1.

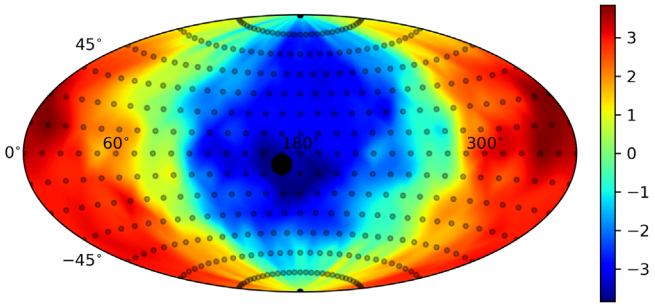

FIG. 8. We show the effect of boosting from $z_{\rm CMB}$ to heliocentric frame. A kinematic dipole is considerably larger.

[1] G. Efstathiou, arXiv:2007.10716.
[2] E. Mortsell, A. Goobar, J. Johansson, and S. Dhawan, arXiv:2105.11461.
[3] N. Aghanim *et al.* (Planck Collaboration), Astron. Astrophys. **641**, A6 (2020).
[4] A. G. Riess, S. Casertano, W. Yuan, L. M. Macri, and D. Scolnic, Astrophys. J. **876**, 85 (2019).
[5] A. G. Riess, S. Casertano, W. Yuan, J. B. Bowers, L. Macri, J. C. Zinn, and D. Scolnic, Astrophys. J. Lett. **908**, L6 (2021).
[6] E. Di Valentino, O. Mena, S. Pan, L. Visinelli, W. Yang, A. Melchiorri, D. F. Mota, A. G. Riess, and J. Silk, Classical Quantum Gravity **38**, 153001 (2021).
[7] C. Krishnan, R. Mohayaee, E. Ó Colgáin, M. M. Sheikh-Jabbari, and L. Yin, Classical Quantum Gravity **38**, 184001 (2021).
[8] S. Vagnozzi, F. Pacucci, and A. Loeb, arXiv:2105.10421.
[9] Potential resolutions to both H_0 and σ_8 tensions may exist outside of GR, e.g. [10].
[10] J. Solà Peracaula, A. Gómez-Valent, J. de Cruz Perez, and C. Moreno-Pulido, Europhys. Lett. **134**, 19001 (2021).
[11] V. Poulin, T. L. Smith, T. Karwal, and M. Kamionkowski, Phys. Rev. Lett. **122**, 221301 (2019).
[12] C. D. Kreisch, F. Y. Cyr-Racine, and O. Doré, Phys. Rev. D **101**, 123505 (2020).
[13] P. Agrawal, F. Y. Cyr-Racine, D. Pinner, and L. Randall, arXiv:1904.01016.
[14] F. Niedermann and M. S. Sloth, Phys. Rev. D **103**, L041303 (2021); **102**, 063527 (2020).
[15] J. C. Hill, E. McDonough, M. W. Toomey, and S. Alexander, Phys. Rev. D **102**, 043507 (2020).
[16] M. M. Ivanov, E. McDonough, J. C. Hill, M. Simonović, M. W. Toomey, S. Alexander, and M. Zaldarriaga, Phys. Rev. D **102**, 103502 (2020).
[17] G. D'Amico, L. Senatore, P. Zhang, and H. Zheng, J. Cosmol. Astropart. Phys. 05 (**2021**) 072.
[18] F. Niedermann and M. S. Sloth, Phys. Rev. D **103**, 103537 (2021).
[19] R. Murgia, G. F. Abellán, and V. Poulin, Phys. Rev. D **103**, 063502 (2021).
[20] T. L. Smith, V. Poulin, J. L. Bernal, K. K. Boddy, M. Kamionkowski, and R. Murgia, Phys. Rev. D **103**, 123542 (2021).
[21] K. Jedamzik, L. Pogosian, and G. B. Zhao, Commun. Phys. **4**, 123 (2021).
[22] W. Lin, X. Chen, and K. J. Mack, Astrophys. J. **920**, 159 (2021).
[23] C. Blake and J. Wall, Nature (London) **416**, 150 (2002).
[24] A. K. Singal, Astrophys. J. Lett. **742**, L23 (2011).
[25] C. Gibelyou and D. Huterer, Mon. Not. R. Astron. Soc. **427**, 1994 (2012).
[26] M. Rubart and D. J. Schwarz, Astron. Astrophys. **555**, A117 (2013).
[27] P. Tiwari and A. Nusser, J. Cosmol. Astropart. Phys. 03 (2016) 062.
[28] J. Colin, R. Mohayaee, M. Rameez, and S. Sarkar, Mon. Not. R. Astron. Soc. **471**, 1045 (2017).
[29] C. A. P. Bengaly, R. Maartens, and M. G. Santos, J. Cosmol. Astropart. Phys. 04 (**2018**) 031.
[30] T. M. Siewert, M. Schmidt-Rubart, and D. J. Schwarz, Astron. Astrophys. **653**, A9 (2021).
[31] N. J. Secrest, S. von Hausegger, M. Rameez, R. Mohayaee, S. Sarkar, and J. Colin, Astrophys. J. Lett. **908**, L51 (2021).
[32] A. K. Singal, arXiv:2106.11968.
[33] A. K. Singal, arXiv:2107.09390.
[34] Indeed, the methods used in these studies make no use of peculiar velocities and are based on distance-independent aberration and Doppler boosting analyses developed within

the framework of special relativity that applies to distributions of sources at high redshifts [35].
[35] G. F. R. Ellis and J. E. Baldwin, Mon. Not. R. Astron. Soc. **206**, 377 (1984).
[36] K. Migkas, G. Schellenberger, T. H. Reiprich, F. Pacaud, M. E. Ramos-Ceja, and L. Lovisari, Astron. Astrophys. **636**, A15 (2020).
[37] K. Migkas, F. Pacaud, G. Schellenberger, J. Erler, N. T. Nguyen-Dang, T. H. Reiprich, M. E. Ramos-Ceja, and L. Lovisari, Astron. Astrophys. **649**, A151 (2021).
[38] S. Yeung and M. C. Chu, arXiv:2201.03799 [Phys. Rev. D (to be published)].
[39] K. C. Wong, S. H. Suyu *et al.* (H0LiCOW collaboration), Mon. Not. R. Astron. Soc. **498**, 1420 (2020).
[40] M. Millon, A. Galan, F. Courbin, T. Treu, S. H. Suyu, X. Ding, S. Birrer, G. C. F. Chen, A. J. Shajib, D. Sluse *et al.*, Astron. Astrophys. **639**, A101 (2020).
[41] J. P. Huchra, L. M. Macri, K. L. Masters, T. H. Jarrett, P. Berlind, M. Calkins, A. C. Crook, R. Cutri, P. Erdogdu, E. Falco *et al.*, Astrophys. J. Suppl. Ser. **199**, 26 (2012).
[42] It may be a coincidence that the $H_0 \sim 74$ km/s/Mpc of DES lens [43] is aligned with the Horologium-Reticulum supercluster. However, the 2MRS catalog is magnitude-limited at $K_s = 11.75$ and therefore can barely reach the brightest galaxies beyond $cz \sim 15,000$ km/s and the clusters that make up Horologium-Reticulum appear to be closer to $cz \sim 20,000$ km/s [44].
[43] A. J. Shajib *et al.* (DES Collaboration), Mon. Not. R. Astron. Soc. **494**, 6072 (2020).
[44] M. C. Fleenor, J. A. Rose, W. A. Christiansen, M. Johnston-Hollitt, R. W. Hunstead, M. J. Drinkwater, and W. Saunders, Astron. J. **131**, 1280 (2006).
[45] M. Kowalski *et al.* (Supernova Cosmology Project), Astrophys. J. **686**, 749 (2008).
[46] R. Cooke and D. Lynden-Bell, Mon. Not. R. Astron. Soc. **401**, 1409 (2010).
[47] D. Scolnic *et al.*, Astrophys. J. **859**, 101 (2018).
[48] Since the errors on H_0 from the lenses are non-Gaussian we use the approximation $\sigma = \frac{1}{2}(2\sigma_1\sigma_2/(\sigma_1+\sigma_2) + \sqrt{\sigma_1\sigma_2})$.
[49] B. Javanmardi, C. Porciani, P. Kroupa, and J. Pflamm-Altenburg, Astrophys. J. **810**, 47 (2015).
[50] H. Ghodsi, S. Baghram, and F. Habibi, J. Cosmol. Astropart. Phys. 10 (2017) 017.
[51] C. A. P. Bengaly, U. Andrade, and J. S. Alcaniz, Eur. Phys. J. C **79**, 768 (2019).
[52] U. Andrade, C. A. P. Bengaly, J. S. Alcaniz, and B. Santos, Phys. Rev. D **97**, 083518 (2018).
[53] X. Yang, F. Y. Wang, and Z. Chu, Mon. Not. R. Astron. Soc. **437**, 1840 (2014).
[54] H. K. Deng and H. Wei, Eur. Phys. J. C **78**, 755 (2018).
[55] Z. Chang, D. Zhao, and Y. Zhou, Chin. Phys. C **43**, 125102 (2019).
[56] R. Mohayaee, M. Rameez, and S. Sarkar, arXiv:2003.10420.
[57] J. Colin, R. Mohayaee, S. Sarkar, and A. Shafieloo, Mon. Not. R. Astron. Soc. **414**, 264 (2011).
[58] S. Appleby, A. Shafieloo, and A. Johnson, Astrophys. J. **801**, 76 (2015).
[59] P. d. Ferreira and M. Quartin, Phys. Rev. Lett. **127**, 101301 (2021).
[60] We made use of the Open Supernova Catalog [61] to identify 18 missing $\mathcal{R}$, $\mathcal{D}$ entries in the Pantheon data.
[61] J. Guillochon, J. Parrent, L. Z. Kelley, and R. Margutti, Astrophys. J. **835**, 64 (2017).
[62] D. J. Schwarz and B. Weinhorst, Astron. Astrophys. **474**, 717 (2007).
[63] C. Krishnan, E. Ó Colgáin, M. M. Sheikh-Jabbari, and T. Yang, Phys. Rev. D **103**, 103509 (2021).
[64] It is easy to increase the number of points in this grid and we expect that it will not greatly change our results.
[65] We find that removing the off-diagonal systematic uncertainties does not greatly affect our quoted significances.
[66] A. G. Riess, W. Yuan, L. M. Macri, D. Scolnic, D. Brout, S. Casertano, D. O. Jones, Y. Murakami, L. Breuval, T. G. Brink *et al.*, arXiv:2112.04510.
[67] E. R. Peterson, W. D'Arcy Kenworthy, D. Scolnic, A. G. Riess, D. Brout, A. Carr, H. Courtois, T. Davis, A. Dwomoh, D. O. Jones *et al.*, arXiv:2110.03487.
[68] R. G. Cai, Z. K. Guo, L. Li, S. J. Wang, and W. W. Yu, Phys. Rev. D **103**, L121302 (2021).
[69] A. G. Riess, R. P. Kirshner, B. P. Schmidt, S. Jha, P. Challis, P. M. Garnavich, A. A. Esin, C. Carpenter, R. Grashius, R. E. Schild *et al.*, Astron. J. **117**, 707 (1999).
[70] S. Jha, R. P. Kirshner, P. Challis, P. M. Garnavich, T. Matheson, A. M. Soderberg, G. J. M. Graves, M. Hicken, J. F. Alves, H. G. Arce *et al.*, Astron. J. **131**, 527 (2006).
[71] M. Hicken, W. M. Wood-Vasey, S. Blondin, P. Challis, S. Jha, P. L. Kelly, A. Rest, and R. P. Kirshner, Astrophys. J. **700**, 1097 (2009).
[72] M. Hicken, P. Challis, S. Jha, R. P. Kirsher, T. Matheson, M. Modjaz, A. Rest, and W. M. Wood-Vasey, Astrophys. J. **700**, 331 (2009).
[73] M. Hicken, P. Challis, R. P. Kirshner, A. Rest, C. E. Cramer, W. M. Wood-Vasey, G. Bakos, P. Berlind, W. R. Brown, N. Caldwell *et al.*, Astrophys. J. Suppl. Ser. **200**, 12 (2012).
[74] C. Contreras, M. Hamuy, M. M. Phillips, G. Folatelli, N. B. Suntzeff, S. E. Persson, M. Stritzinger, L. Boldt, S. Gonzalez, W. Krzeminski *et al.*, Astron. J. **139**, 519 (2010).
[75] G. Folatelli, M. M. Phillips, C. R. Burns, C. Contreras, M. Hamuy, W. L. Freedman, S. E. Persson, M. Stritzinger, N. B. Suntzeff, K. Krisciunas *et al.*, Astron. J. **139**, 120 (2010).
[76] M. D. Stritzinger, M. M. Phillips, L. N. Boldt, C. Burns, A. Campillay, C. Contreras, S. Gonzalez, G. Folatelli, N. Morrell, W. Krzeminski *et al.*, Astron. J. **142**, 156 (2011).
[77] J. A. Frieman, B. Bassett, A. Becker, C. Choi, D. Cinabro, D. F. DeJongh, D. L. Depoy, M. Doi, P. M. Garnavich, C. J. Hogan *et al.*, Astron. J. **135**, 338 (2008).
[78] R. Kessler, A. Becker, D. Cinabro, J. Vanderplas, J. A. Frieman, J. Marriner, T. M. Davis, B. Dilday, J. Holtzman, S. Jha *et al.*, Astrophys. J. Suppl. Ser. **185**, 32 (2009).
[79] M. Sako *et al.* (SDSS Collaboration), Publ. Astron. Soc. Pac. **130**, 064002 (2018).
[80] A. Rest, D. Scolnic, R. J. Foley, M. E. Huber, R. Chornock, G. Narayan, J. L. Tonry, E. Berger, A. M. Soderberg, C. W. Stubbs *et al.*, Astrophys. J. **795**, 44 (2014).
[81] D. Scolnic, A. Rest, A. Riess, M. E. Huber, R. J. Foley, D. Brout, R. Chornock, G. Narayan, J. L. Tonry, E. Berger *et al.*, Astrophys. J. **795**, 45 (2014).
[82] A. Conley *et al.* (SNLS Collaboration), Astrophys. J. Suppl. Ser. **192**, 1 (2011).

[83] M. Sullivan *et al.* (SNLS Collaboration), Astrophys. J. **737**, 102 (2011).
[84] N. Suzuki *et al.* (Supernova Cosmology Project), Astrophys. J. **746**, 85 (2012).
[85] A. G. Riess *et al.* (Supernova Search Team), Astrophys. J. **607**, 665 (2004).
[86] A. G. Riess, L. G. Strolger, S. Casertano, H. C. Ferguson, B. Mobasher, B. Gold, P. J. Challis, A. V. Filippenko, S. Jha, W. Li *et al.*, Astrophys. J. **659**, 98 (2007).
[87] S. A. Rodney, A. G. Riess, L. G. Strolger, T. Dahlen, O. Graur, S. Casertano, M. E. Dickinson, H. C. Ferguson, P. Garnavich, B. Hayden *et al.*, Astron. J. **148**, 13 (2014).
[88] O. Graur, S. A. Rodney, D. Maoz, A. G. Riess, S. W. Jha, M. Postman, T. Dahlen, T. W. S. Holoien, C. McCully, B. Patel *et al.*, Astrophys. J. **783**, 28 (2014).
[89] A. G. Riess, S. A. Rodney, D. M. Scolnic, D. L. Shafer, L. G. Strolger, H. C. Ferguson, M. Postman, O. Graur, D. Maoz, S. W. Jha *et al.*, Astrophys. J. **853**, 126 (2018).
[90] R. Watkins, H. A. Feldman, and M. J. Hudson, Mon. Not. R. Astron. Soc. **392**, 743 (2009).
[91] G. Lavaux, R. B. Tully, R. Mohayaee, and S. Colombi, Astrophys. J. **709**, 483 (2010).
[92] C. Magoulas, C. Springob, M. Colless, J. Mould, J. Lucey, P. Erdogdu, and D. Jones, *Proceedings of the International Astronomical Union* 11(S308), 336 (2014).
[93] C. Howlett, K. Said, J. R. Lucey, M. Colless, F. Qin, Y. Lai, R. B. Tully, and T. M. Davis, arXiv:2201.03112.
[94] O. Luongo, M. Muccino, E. Ó Colgáin, M. M. Sheikh-Jabbari, and L. Yin, arXiv:2108.13228.
[95] M. Rameez, arXiv:1905.00221.
[96] M. Rameez and S. Sarkar, Classical Quantum Gravity **38**, 154005 (2021).
[97] D. Rubin and J. Heitlauf, Astrophys. J. **894**, 68 (2020).
[98] W. Rahman, R. Trotta, S. S. Boruah, M. J. Hudson, and D. A. van Dyk, arXiv:2108.12497.
[99] M. L. McClure and C. C. Dyer, New Astron. **12**, 533 (2007).